

# CFD Analysis on the Effect of Vortex Generator on Sedan Car using ANSYS Software

Muhammad Pirdaus Ismail<sup>1\*</sup>, Izuan Amin Ishak<sup>1</sup>, Nor Afzanizam Samiran<sup>1</sup>, Ahmad Faiz Mohammad<sup>2</sup>, Zuliazura Mohd Salleh<sup>1</sup>, Nofrizalidris Darlis<sup>1</sup>

<sup>1</sup>Department of Mechanical Engineering Technology, Faculty of Engineering Technology, Universiti Tun Hussein Onn Malaysia, 86400 Pagoh, Johor, MALAYSIA

<sup>2</sup>Department of Mechanical Precision Engineering, Malaysia-Japan International Institute of Technology (MJIIT), Universiti Teknologi Malaysia (UTM), Jalan Sultan Yahya Petra, 54100, Kuala Lumpur, MALAYSIA

\*Corresponding author

DOI: <https://doi.org/10.30880/ijie.2022.14.01.008>

Received 24 November 2020; Accepted 28 May 2021; Available online 07 March 2022

**Abstract:** Nowadays, the demand for a high-speed car increases in which vehicle stability and fuel economy are the primary concern. The vehicle's aerodynamics plays a crucial role as it influences the overall performance of the vehicles. In the exploration of car aerodynamics, it involves studying various forces that act on a car while moving on the road, i.e., drag force, lift force. The leading causes of aerodynamic drag for automotive vehicles are the flow separation at the vehicles' rear end. By reducing the drag force, it is possible to increase the fuel economy. The research is focused on the effect of a vortex generator (VG) on a sedan car aerodynamics. The objective is to simulate fluid flow analysis for a sedan car that uses VG and without VG, to assess the effect of a different configuration of VG and the impact of a varying number of VG mounted on a sedan car in terms of flow pattern development and coefficient of drag ( $C_d$ ). This study is conducted using two identical sedan car models, i.e., with VG and without VG. The flow around the vehicle has been considered incompressible. It is obtained by solving the incompressible form of the Reynolds Navier-Stokes (RANS) equations combined with the  $k-\epsilon$  turbulence model. The simulation is run for different configuration of VG that acquire different radius of fillet, i.e., VG-1 (5 mm), VG-2 (30 mm) and VG-3 (50 mm) and for different number of VG that is mounted on a sedan car, i.e., 0 VG, 1 VG, 3 VG, 5 VG, 7 VG, and 9 VG. The data and results taken from this simulation show that the smallest fillet radius of VG, i.e., VG-1 (5 mm), is the best VG to be used on a sedan car. The results also show that, as the number of VGs increases, the drag coefficient is decreased. Hence, the best number of VGs to be used on a sedan car are nine VGs.

**Keywords:** Aerodynamics, vortex generator, flow separation, coefficient of drag

## 1. Introduction

Fuel consumption is the primary concern in automotive development, especially for energy resources conservation and protecting the global environment. Most of the car nowadays are designed to achieve an ideal aerodynamic so that cars will have excellent performance. Improvement in the vehicle's aerodynamics is one of the vehicle developers' critical concerns to advance the fuel economy [1]. Aerodynamics helps to decrease the drag force, makes cars more stabilised, and reduces fuel consumption. Pressure drag is the pressure difference in the front and rear end of the vehicle, and as the ground vehicles are concerned, pressure drag contributes almost 90 % of the total drag [2]. Some car has a body shape that is rather aerodynamically bluff for which flow separation occurs at its rear end. The aerodynamic bluntness of a passenger car body when expressed by the drag coefficient,  $C_d$  is generally between 0.2 and 0.5 [3]. For more bluff cubic objects, it is greater than 1.0, and for the least bluff shape, it is less than 0.1 [3]. Flow separation

control remains extremely important for many practical fluid mechanics applications due to large energy losses often associated with the boundary-layer separation [4]. Reducing flow separation is important on a car; hence, it increasing car performance by drag reduction. Some method was founded to control the flow over the vehicle by adding aerodynamic devices such as Vortex generator (VG). Vortex Generators are passive aerodynamic devices that can be categorised as boundary- layer manipulators [5]. A VGs function is to energise an opposing pressure gradient boundary layer and enhance its mixing, which is about to separate, by conveying high momentum fluid from the outer part of the boundary layer down to the low momentum zone closer to the wall [5]. According to investigations, it is concluded that the vortex generators modifies the inner structure of the boundary layer, making it more resistant to separation; hence, it preventing flow separation at the rear of the car [5,6]. Mostly VGs are used in sedan type cars instead of hatchback type cars because the drag coefficient and lift coefficient for the hatchback design is much lower than the sedan design [7].

## 1.1 Aerodynamics

Aerodynamics is the study of how air is associated with moving bodies. It is the study of forces and the resulting motion of objects through the air. Understanding the movement of air around an object enables the calculation of forces and moments acting on the object. Typical properties calculated for a flow field include velocity, pressure, density, and temperature as a function of position and time [8]. Aerodynamics is primarily concerned with the lift force and drag force, which are caused by air passing over and around solid bodies. [9]. In automotive, aerodynamics is the study of the streamlined features of street vehicles. Its main objectives are decreasing drag and wind noise, minimising noise emission, and preventing undesired lift forces and other causes for aerodynamic instability at high speeds. For certain racing cars classes, it is also essential to produce down-force; hence, it will improve the traction [10]. Aerodynamic drag is the sum of pressure drag and viscous drag. The pressure drag is caused due to the shear forces acting between the two fluid layers [11]. Pressure drag accounts for more than 80% of the total drag and it is highly dependent on vehicle geometry due to boundary layer separation from rear window surface and formation of wake region behind the vehicle [12]. Aerodynamic drag consists of two main components, which are skin friction drag and pressure drag. Skin friction drag is the resistant force exerted on an object moving in a fluid, and it is caused by the viscosity of fluids and is developed from laminar drag to turbulent drag as a fluid moves on the surface of an object [13]. Drag is comprised primarily of three forces which are frontal pressure that is created when the body of the vehicle pushing air out of the way at the frontal area of vehicle body, the rear vacuum that is occurred when the air not being able to fill the hole left by the vehicle body and the boundary layer that is created by slow-moving air at the surface of the vehicle body. Between these three forces, one can describe most of the airflow interactions with a vehicle body. The equation of coefficient of drag ( $C_d$ ) is shown below where  $F_d$  is represent the drag force,  $\rho$  is density of the fluid,  $V^2$  is flow velocity relative to the object and  $A$  is frontal area

$$C_d = \frac{F_d}{0.5 \rho V^2 A} \quad (1)$$

## 1.2 Types of drag

Drag is generally divided into three, which are a parasitic drag, induced drag, and wave drag. Parasitic drag consisting of pressure drag, skin friction and interference drag. Pressure drag is created due to the shape of the object. The general size and shape of a car body are the most crucial factor in this drag; bodies with larger presented cross-sections will have higher drag than small frontal area or cross-sections [14]. Skin friction drag is produced from the fluid's friction against the "skin" of the object that is moving through it. It arises from the interaction between the skin of the body and the fluid, and is directly related to the wetted surface, the surface area of the body that is in contact with the fluid [13]. Interference drag is generated by the mixing of airflow streamlines between the component airframe, such as the fuselage and wing [15]. Induced drag is caused by the down-flow of the airstream passing over the wing of an aircraft, equal to the lift times the tangent of the induced angle of attack [16]. Wave drag is caused by the air becoming sonic over any portion of the body [14]. In this drag, it is caused by two things which are first, when the air crosses the shock wave, some of the energy is lost as a drag because of the temperature across the shock wave and second when a shock-induced boundary-layer separation increases the drag.

## 1.3 Reynolds Number

The Reynolds number ( $Re$ ) is used to study fluids as they flow. It determines whether a fluid flow is laminar or turbulent [17]. Flowing fluids normally follow along streamlines. If a flow is laminar, fluids will move along smooth streamlines. If the flow is turbulent, these streamlines breakup and the fluid will move irregularly. Turbulent flow creates more friction drag on an aeroplane. However, it also keeps the flow attached over its surface. In general,  $Re$  can be expressed as:

$$Re = \frac{\rho \times V \times L}{\mu} \quad (2)$$

where  $\rho$  is the density of the fluid in  $\text{kg/m}^3$ ,  $V$  is the velocity of the fluid in  $\text{m/s}$ ,  $L$  is the characteristic linear dimension or length of fluid in  $\text{m}$ , and  $\mu$  is the dynamic viscosity of a fluid in  $\text{kg/ms}$  [18].

The relationship between  $Re$  and aerodynamics is the parameter used for viscosity. The  $Re$  expresses the ratio of inertial forces, which is resistant to change or motion to viscous forces. The exact values for when  $Re$  are 'large' or 'small' are not well defined but vary depending on an actual problem. The flow is based on the value of  $Re$ , if  $Re < 2000$ , the flow is called laminar, if  $Re$  value is between 2000 to 4000, it is called transition and if  $Re > 4000$ , the flow is called turbulent [17].

## 1.4 Flow Separation

Fluid climbs the uphill portion of the curved surface without a problem, but it is difficult to remain attached to the surface on the downhill side. When a car travels at high velocities, the fluid streams detach itself from the rear surface of the car body, and this is called flow separation. Flow separation is the point on the surface where the inertia force of the near-wall fluid particle equals the frictional force [19]. It occurs when the boundary layer travels far enough against an adverse pressure gradient that the speed of the boundary layer relative to the object falls almost to zero [20]. Because of friction between the solid surface and the air particles passing over it, the airframes a fluid profile, with stationary air sitting at the purpose of gathering between the fluid and the surface. This profile is also known as the boundary layer. The velocity at that point created to what is called free stream speed as the separation increments from the vehicle's body.

## 1.5 Vortex Generator

Vortex generator is an aerodynamics device that modifies the boundary layer fluid motion by bringing momentum from the outer flow region into the inner flow region of the wall-bounded flow [21]. It consists of small vanes commonly attached to the vehicle surface to reduce the aerodynamic drag. Vortex generator is usually triangular or rectangular vanes inclined at an angle to the incoming flow. These generators are typically dimensioned in relation to the local boundary layer thickness to allow for the best interaction between the generated vortex wake and boundary layer. They are usually placed in groups of two or more upstream of the flow separation area [21].

## 2. Methods

Computational Fluid Dynamics (CFD) is a branch of fluid mechanics that uses numerical analysis and data structures to analyse and solve a problem that involves fluid dynamics and heat transfer [22]. In the study of car aerodynamics, it involves design. Engineers need to conduct a physical test on product prototypes to optimise the design. This method consumes a significant amount of time and money because it requires product prototypes and testing. By using CFD, all things can be analysed, and all necessary data can be obtained in a short time, quick and cost-effective. CFD became a commonly applied tool for generating solutions for fluid flow with or without solid interaction. In CFD analysis, the examination of fluid flow in accordance with its physical properties such as velocity, pressure, temperature, density, and viscosity are conducted. The physical characteristics of the motion of a fluid can usually be described through the fundamental mathematical equations, usually in partial differential form, which governs a process of interest and is often called governing equations in CFD. CFD has become one of the three primary ways or approaches that can be used to solve problems in fluid dynamics or heat transfer [23]. As demonstrated in Figure 2.1, each approach is strongly interlinked and does not lie in isolation

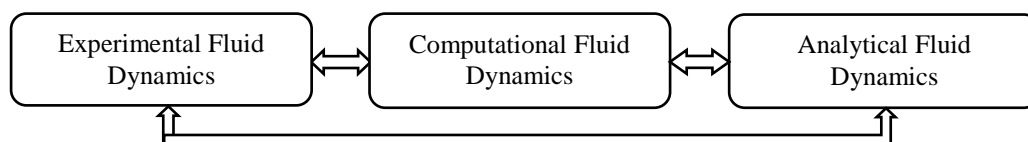


**Fig. 2.1 - Three basic approaches to solve fluid dynamics and heat transfer problems**

The numerical simulations in this study are implemented using the ANSYS software. It contains the broad, physical modelling capabilities needed to model flow, turbulence, heat transfer, and reaction for industrial applications. Fluent also highly scalable to help solve complex, large-model computational fluid dynamics. The solution involving a variety of cases required complex equations and calculations.

### 2.1 Model Description

The model used in this study is a sedan car model based on the Audi A4 B8 year 2015 car geometry. This model is designed by using SOLIDWORKS 2018 software by referring to the actual geometry and dimension of car model blueprint. The car model is used as a reference for this study to analyse the flow pattern around a car model and its drag

coefficient when it is mounted with a vortex generator. Figure 2.2 shows the numerical model of the sedan car without vortex generator, and Table 2.1 shows the detail dimension for this car model.

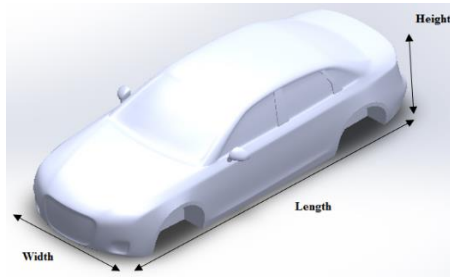


**Fig. 2.2 - Sedan car numerical model**

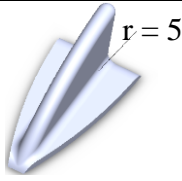
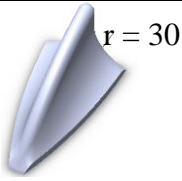
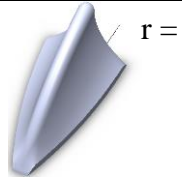
**Table 2.1 - Dimension of sedan car**

Configuration of sedan car model	Dimension (mm)
Length	4690
Width	1815
Height	1203

### 2.2 Design of Vortex Generator

In this study, three different VG is used. The VG was designed using SOLIDWORKS software. The size of the VG is selected based on the boundary layer thickness at the roof rear end immediately in front of the separation point, which is about 30 mm [24]. Therefore, the optimum height for the VG is found to be up to approximately 30 mm. Table 2.2 shows the three vortex VG that is similar in shape but acquire different in the radius of fillet, i.e.  $r = 5$ ,  $r = 30$   $r = 50$ . The radius of fillet on the side of VG was chosen as a variable in this study to varying the shape of VG. Different value radius of fillet affecting the shape of VG as well and will result different value of  $C_d$  in the simulation.

**Table 2.2 - Design of vortex generator**

VG-1	VG-2	VG-3
		
<b>Dimension (mm)</b>	<b>Dimension (mm)</b>	<b>Dimension (mm)</b>
Length= 100	Length= 100	Length= 100
Width= 50	Width= 50	Width= 50
Height= 30	Height= 30	Height= 30
Thickness= 15	Thickness= 15	Thickness= 15
$r = 5$	$r = 30$	$r = 50$

### 2.3 Location of Vortex Generator

As to the location of vortex generators, a point immediately upstream of the flow separation point exists, and a position at an optimum distance of 130 mm in front of the roof end was selected as shown in Figure 2.3 (a). Figure 2.3 (b) show nine VGs with an equal spacing which is about 74 mm distance for each VG. Figure 2.3 (c) shows a sedan car model mounted with nine vortex generators on top of the roof at the rear end with equal spacing. Vortex generators are assembled on the top roof of a sedan car model by using SOLIDWORKS 2018 software. By using the linear pattern function in SOLIDWORKS, it allows to create equal spacing between each VG. The total width to mount the VG is 1042 mm. The selection of how many VG to be mounted on the rear car roof are referred from the past studies. Based on previous researchers, the optimum number of VG to be mounted on the rear car roof is 9 VGs [25].

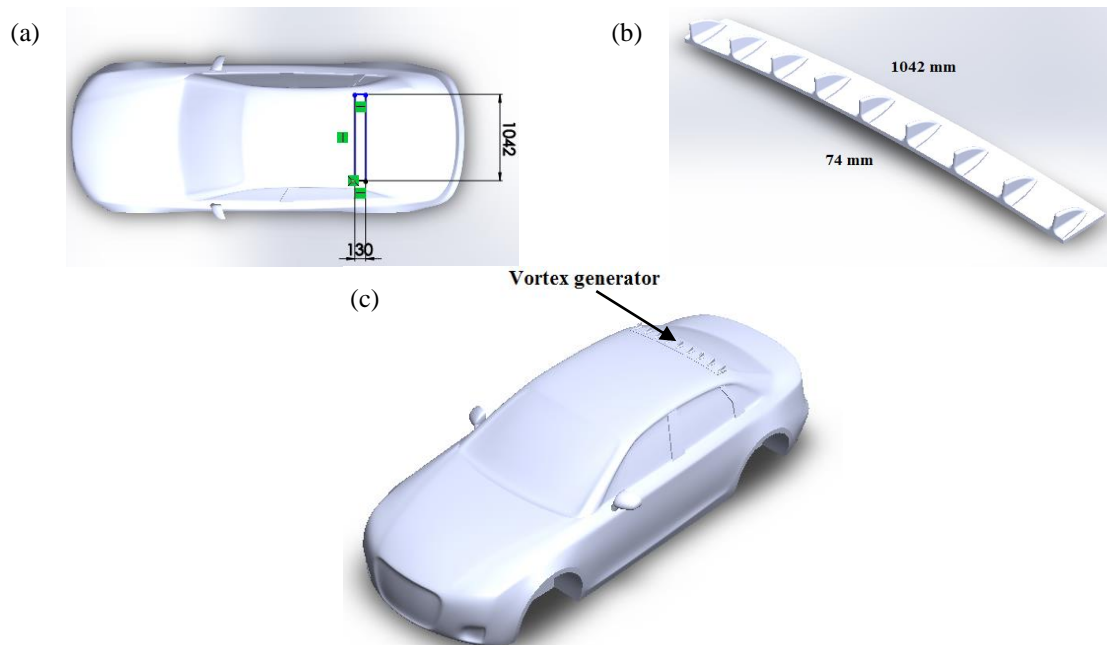


**Fig. 2.3 - (a) location of vortex generator to be mounted; (b) nine of vortex generator with equal spacing; (c) car model with vortex generator**

## 2.4 Step Performing the Simulation

The first step before running the simulation is to create a 3D model. In this project, a 3D model is imported from SOLIDWORKS to ANSYS. The model creation is generated in ANSYS, and the fluid domain is created before the meshing process. Fluid domain or enclosure is used by analysis tools to simulate fluid. The size of the enclosure is shown in Figure 2.4, i.e.  $W = 1.8$  m,  $H = 1.2$  m,  $L = 4.69$  m.

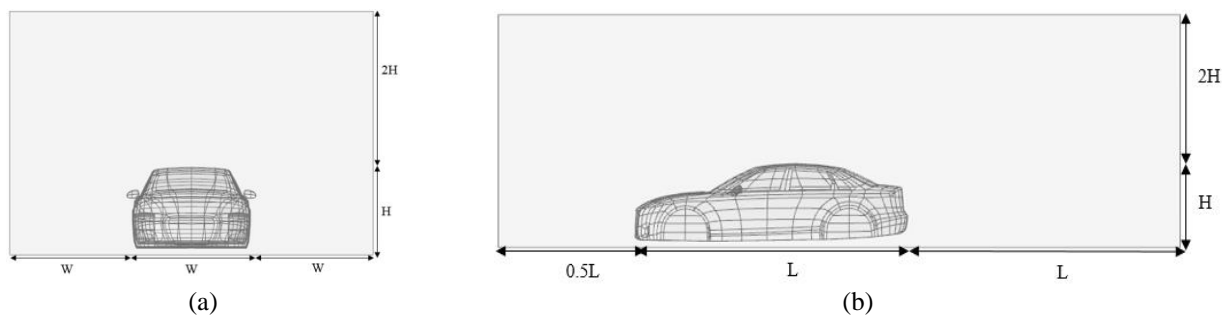


**Fig. 2.4 - Size of enclosure; (a) front view, (b) side view**

Next is the meshing process, meshing is the process discretisation model into several elements [26], and it is the most crucial process in simulation in order to get a good result. The quality of mesh defines the accuracy of the results. A tetrahedral mesh is used for the project. In the process of meshing, the position of the inlet, outlet and wall of the model are determined. Figure 2.5 show the complete mesh of the enclosure.

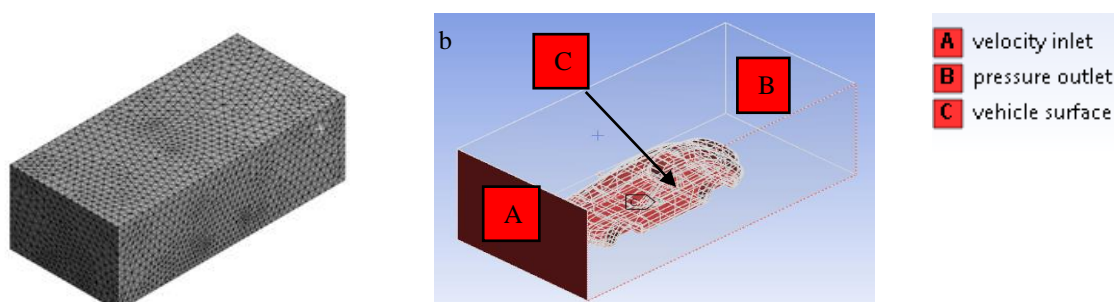


**Fig. 2.5 - (a) Complete mesh of the enclosure; (b) Position of velocity inlet, pressure outlet & vehicle surface**

The model is meshed with the tetrahedral method due to its simple model design. The mesh is set automatic for the global mesh and manually for the local mesh. The size of mesh quadrant is set to 0.2 meters, and the smoothing sensitivity of the meshing is high. The total number of meshes is equal to 761168 elements and 72632 nodes. After the process of mesh completed, the boundary conditions of the model such as velocity inlet, pressure outlet, vehicle surface, the roughness of the wall and the type of flow are set in setup process as shown in Table 2.3. It is a condition that is required to be satisfied at all or part of the boundary of a region in which a set of differential conditions is to be solved. Setting the boundary condition is a must to obtain the correct results for the CFD analysis [27]. In this study, the Reynolds number used is  $Re = 8.8 \times 10^5$ . This value is chosen because of it will results the same value of  $C_d$  in the simulation if the  $Re$  exceed more than  $8.8 \times 10^5$ . Hence, this value is chosen for this study. The type of analysis for this research is external flow types which is only include the external force exerted on the surface of the sedan car like drag force and pressure. The medium of fluid is air which is the actual condition as in real life.

**Table 2.3 - Boundary conditions**

Detail	Boundary Condition	Value
Inlet	Velocity inlet	100 km/h
Outlet	Pressure outlet	0 Pa (gauge)
Wall	Wall boundary	Free slip wall
Vehicle surface	Wall boundary	No-slip wall
Reference	Ambient	101.325 kPa

When the pre-processing is completed, the simulation is ready to run to get the data and results needed. In this study, the simulation is running in total nine times which is one with a car model without VG, three times for different shape of VG and five times for the different number of VG mounted on a sedan car, i.e. 1 VG, 3 VG, 5 VG, 7 VG, 9 VG. The data obtained from this simulation is used for further analysis.

### 3. Results and Discussion

#### 3.1 Effect of Different Shapes of Vortex Generator

Figure 3.1 shows the result of the coefficient of drag ( $C_d$ ) against different shapes of VG. Result show, as the VG fillet radius is increased, the  $C_d$  is also increased. VG-1 with a fillet radius 5 mm results in the  $C_d$  equal to 0.312, while the VG-2 and VG-3 which acquire 30 mm and 50 mm of fillet radius cause the  $C_d$  to increases up to 0.327 and 0.332 respectively. Therefore, it can be considered that the VG with the lowest fillet radius is the best shapes of VG to be used on the cars.

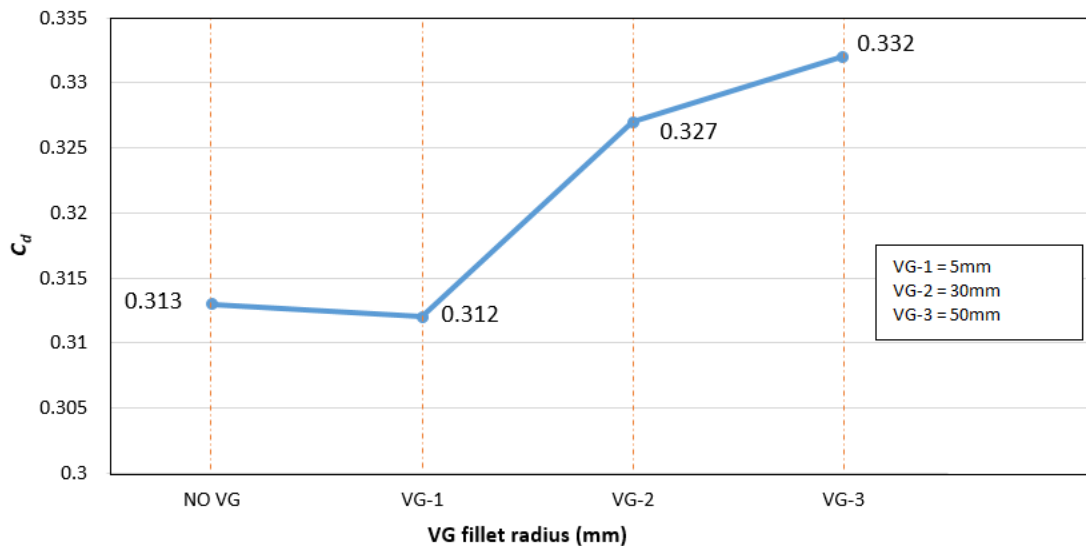


**Fig. 3.1 - Coefficient of drag ( $C_d$ ) against different shapes of vortex generator (VG)**

#### 3.2 Effect of a Varying Number of Vortex Generator

The best VG based on the fillet radius, i.e. VG-1 which has acquired the lowest  $C_d$  is used for further investigation this section. Figure 3.2 shows the effect of varying numbers of VG on the coefficient of drag ( $C_d$ ). The value of  $C_d$  is taken for a sedan car model that is mounted with 1 VG, 3VGs, 5 VGs, 7 VGs, and 9 VGs.



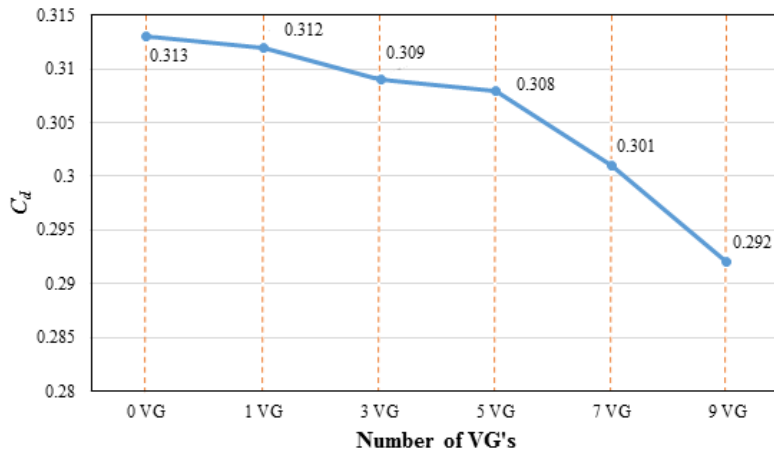


**Fig. 3.2 - Coefficient of drag ( $C_d$ ) against different number of vortex generator**

As shown in Figure 3.2, the result indicates that the  $C_d$  is decreased as the number of VGs increases. For a car without VG, the  $C_d$  value is equal to 0.313. Then, when 1 VG is used, the  $C_d$  is reduced to 0.312. In this simulation, the lowest  $C_d$  value obtained is equal to 0.292 by using 9 VGs. This is equivalent to a 6.7% improvement of  $C_d$  when 9 VGs are used as compared to a car that is not installed with VG. Results also show that the value of  $C_d$  for 3 VGs and 5 VGs are almost the same which is equal to 0.309 and 0.308 respectively which is only 0.001 differences between them. Then, the value of  $C_d$  is decreased from 0.308 to 0.301 when 7 VGs are used, and it continues to drop to 0.292 when two more VGs are added that make the total of VGs used are 9 VGs. Therefore, it can be deduced that the best number of VGs to be used on a sedan car are 9 VGs. It can also be visualised that the effect of the number of VGs starts to become more apparent once more than 5 VGs are mounted on the car.

### 3.3 Flow Structure between Sedan Car that Uses Different Shapes of VG

Figure 3.3 shows the comparison of flow structure analysis between sedan cars that use different shapes of VG i.e. VG-1 (5 mm), VG-2 (30 mm), and VG-3 (50 mm).

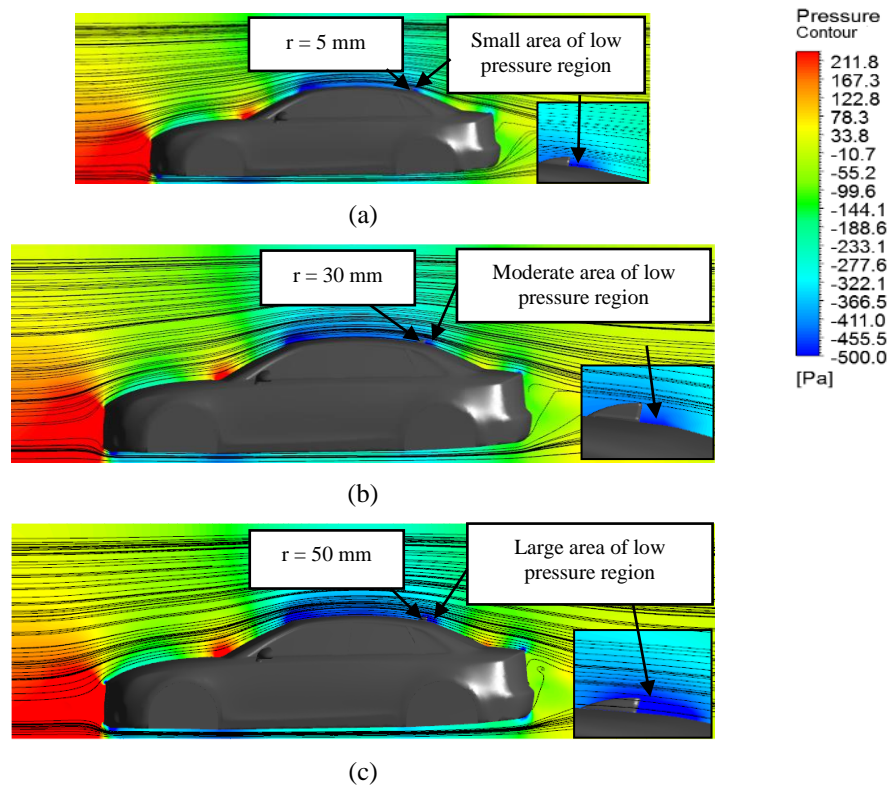


**Fig. 3.3 - Streamline superimposed on the pressure contour for the sedan car mounted with different shapes of VG; (a) VG-1 (b) VG-2 (c) VG-3**

For VG-1, it can be seen that there is a small area region of low pressure (dark blue colour) after the air passes through it, while VG-2 has a slightly bigger of the low-pressure region compared to VG-1. Lastly is VG-3, which has a larger size of the low-pressure region after the air passes through it. From this figure, as the VG fillet radius increases, the size of the low-pressure region also increases. This low-pressure region causes vortex formation in it, thus, creates the separation of flow that results in increasing the  $C_d$  value.

### 3.4 Flow Structure of Sedan Car that is Mounted with a Different Number of VG

Figures 3.4 (a) shows the pressure contour of the entire vehicle body with 1 VG and Figures 3.4 (b)-(f) show the comparison of flow structure between sedan car that is mounted with 1 VGs, 3 VGs, 5 VGs, 7 VGs and 9 VGs. From the figures, as the free stream flow approaches the sedan car's front area, the flow, particularly along the central axis, is forced to move away from the body. A stagnation point appears at the central point of the model, which can also be depicted clearly in Figure 3.4. In theory, a stagnation point occurs when the local velocity of a fluid is zero and consequently result in the highest pressure area, as shown in Figure 3.4 (a). Figure 3.4 (a)-(b) shows the pressure contour of the entire vehicle body and its surroundings when mounted with one VG. From the figure, it shows that the pressure on the surface of the VG and its surroundings is lower due to high velocity of air stream in that region. Figure 3.4 (c) shows the velocity streamline of a sedan car model that is mounted with 3 VGs. From this figure, there is not so much difference that can be seen in the flow structures compared to a sedan car that is mounted with 1 VG. However, a small difference can be seen in the high air stream velocity distance after it passes through VG ( $A = 1/5 H$ ) before it starts to lose its velocity due to friction at point  $B$ . For the wake structure pattern, this figure shows that the wake's length is  $C = 0.8 H$ . Figure 3.4 (d) shows the result of streamline for a sedan car model that is mounted with 5 VGs. In this case, the air stream velocity remains a bit longer at high speed (point  $A$ ) compared to the situation shown in Figure 3.4 (c). After the airflow passes through 5 VGs, the air travels at high speed before it loses its velocity due to friction at point  $B$ , which is after it travels about  $A = 1/3 H$ . The length of the wake structure continues to decrease as the increasing number of VGs. This figure shows that the wake structure's length is about  $C = 1/2 H$ . Figure 3.4 (e) shows that the length of  $A$  increases compared to Figure 3.4 (d). The air move in high velocity after it passes through 7 VGs before it loses its velocity after travels about  $A = 2.3/5 H$ . In this situation, less separation occurs due to low pressure at the rear windshield caused by the air stream's high velocity. The wake structure length is smaller than a car mounted with 5 VGs, which is about  $C = 0.4 H$ .

Lastly, Figure 3.4 (f) shows the velocity streamlines of a model mounted with 9 VGs. This figure shows that the streamline pattern is almost similar to the streamline pattern shown in Figure 3.4 (e). Still, a slight difference in the structure length at the rear end of the car, which is about  $C = 0.3 H$ . The air velocity remains high after passes through 9 VGs causes the air to remain attached to the rear windshield and the car body surface. The airflow starting to lose its velocity after it travels about  $A = 1/2 H$ . Thus, no separation of flow occurs in the  $A$  region. This figure clearly shows that the airflow is moving to the ground, resulting in the small wake structures at the rear end. Hence, this causes a reduction in  $C_d$ .

## 4. Conclusion

In this research, investigations on the aerodynamics characteristic inclusive of aerodynamic loads and flow structure of a sedan car model mounted with different shapes and numbers of vortex generators are assessed. As for the main findings, the effects of different shapes and the varying number of vortex generators on a sedan car towards the coefficient of drag ( $C_d$ ) value and flow structure is explored and presented. Based on the results, the different configurations of VG have a significant impact on the  $C_d$  value. VG-3 has the highest  $C_d$ , while VG-1 has the lowest  $C_d$ . This finding explained when the fillet radius of VG increases, the drag force is increased too. The result also shows that, as the number of VG increases, the  $C_d$  is increased. The result of  $C_d$  for 9 VGs is the lowest compared to others which is equal to 0.292. In terms of flow structure, the result proves that the VG can delay the flow separation. This finding is presented, which explained the detail about air stream velocity after it travels passes through VGs. The air stream is necessary to remain in high velocity so that it can remain attached to the vehicle body surfaces. Hence, flow separation will not occur. This finding shows the difference of 'A' length, representing the air stream's high velocity after it passes through VG. In this case, the length of 'A' is equal to half of the length of  $H$  for 9 VGs. Compared to other results, this is the most extended area or region of the air stream that travels in high velocity before it starts to lose its velocity due to friction at 'B'. In conclusion, the result shows that the 9 VGs are the best number of VG to be mounted on a sedan car. Hence, this proposal of implementing VG with fillet radius = 5 mm and 9 VGs can potentially reduce  $C_d$ 's value by 5.81 % compared with a car without VG.



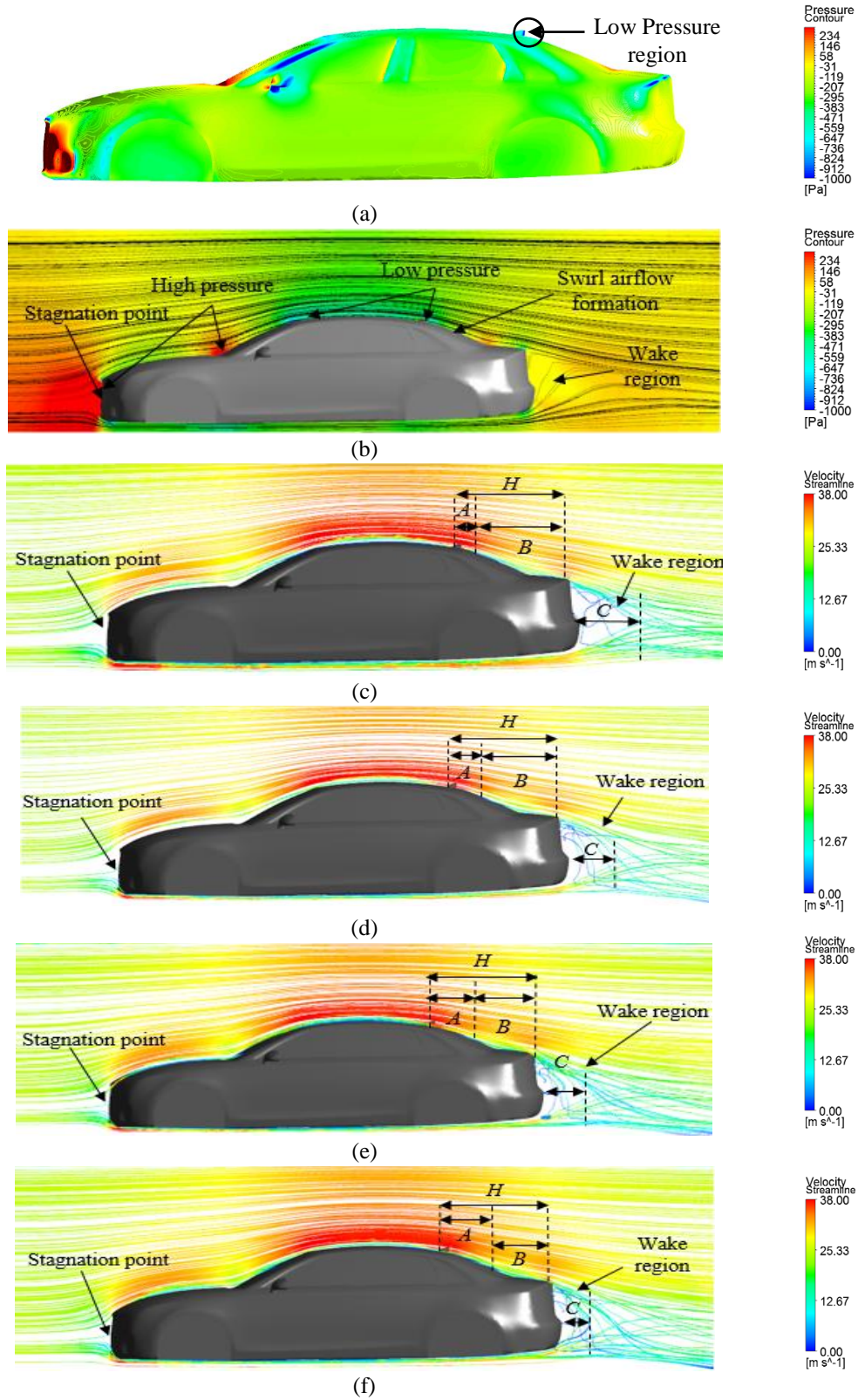


**Fig. 3.4 - (a) Pressure contour of the entire vehicle body with 1 VG, Velocity streamline on the sedan car; (b) 1 VG; (c) 3 VG; (d) 5 VG; (e) 7 VG; (f) 9 VG**

## Acknowledgement

This research was financially supported by Universiti Tun Hussein Onn Malaysia under UTHM Contract Grant (H523). The author would also like to thank the Faculty of Engineering Technology, Universiti Tun Hussein Onn Malaysia for providing the necessary research facility for this study.

## References

- [1] D. Sagar, A. R. Paul, R. R. Upadhyay, and A. Jain, "Aerodynamic Effects of Rear Spoiler and Vortex Generators on Passenger Cars," *Proceedings of 5th International Conference on Theoretical, Applied, Computational and Experimental Mechanics (ICTACEM-2010)*, no. 311, pp. 760–762, 2010.
- [2] P. Adarsh, A. G. Cherian, and D. R. Kumar, "Numerical Investigation of Drag on a Trailing Aerodynamic Sedan Car," *International Journal of Mechanical and Production Engineering (IJMPE)*, vol. 2, no. 4, pp. 81–86, 2014.
- [3] Kumar, Mohan & Dubey, Anoop & Chheniya, Shashank & Jadhav, Amar, "Effect of Vortex Generators on Aerodynamics of a Car: CFD Analysis," *International Journal of Innovations in Engineering and Technology (IJIET)*, vol. 2, no. 1, pp. 137-144, 2013
- [4] John C. Lin, "Review of Research on Low-Profile Vortex Generators to Control Boundary- Layer Separation", *Progress in Aerospace Sciences*, pp. 389-420, No. 38, 2002.
- [5] P. Gopal, T. Senthikumar, and C. Rameshkumar, "Aerodynamic drag reduction in a passenger vehicle using vortex generator with varying yaw angles," *ARPJ. Eng. Appl. Sci.*, vol. 7, no. 9, pp. 1180–1186, 2012.
- [6] S. Xue, B. Johnson, D. Chao, A. Sareen, and C. Westergaard, "Advanced aerodynamic modeling of vortex generators for wind turbine applications," *Eur. Wind Energy Conf. Exhib. 2010, EWEC 2010*, vol. 5, no. October 2016, pp. 3721–3731, 2010.
- [7] M. K. A. Bin Salleh, "Simulation and Analysis Drag and Lift Coefficient Between Sedan and Hatchback Car," *Thesis submitted for the degree of Bachelor of Mechanical Engineering*, Universiti Malaysia Pahang, November, 2009.
- [8] P. N. Selvaraju, K. M. Parammasivam, S. Shankar, and G. Devaradjane, "Analysis of drag and lift performance in sedan car model using CFD," *J. Chem. Pharm. Sci.*, vol. 7, no. 7, pp. 429–435, 201
- [9] Jim Lucas, "What is Aerodynamics," Retrieved from <https://www.livescience.com/47930-what-is-aerodynamics.html>, September 2014.
- [10] Le Good, Geoff & Garry, Kevin. "On the Use of Reference Models in Automotive Aerodynamics", *SAE 2004 World Congress & Exhibition*, pp. 28, 2004.
- [11] S. Hetawal, M. Gophane, B. K. Ajay, and Y. Mukkamala, "Aerodynamic study of formula SAE car," *Procedia Eng.*, vol. 97, pp. 1198–1207, 2014
- [12] M. N. Sudin, M. A. Abdullah, S. A. Shamsuddin, F. R. Ramli, and M. M. Tahir, "Review of research on vehicles aerodynamic drag reduction methods," *Int. J. Mech. Mechatronics Eng.*, vol. 14, no. 2, pp. 35–47, 2014.
- [13] C. K. Chear and S. S. Dol, "Vehicle aerodynamics: Drag reduction by surface dimples," *Int. J. Mech. Mechatronics Eng.*, vol. 9, no. 1, pp. 202–205, 2015.
- [14] J. Lella, "Effect of Vortex Generators on a Streamlined Sports car Effect of Vortex Generators On Drag of A Car", *Project Report submitted in partial fulfilment of the requirements for the award of the degree of Bachelor of Technology*, July, 2015.
- [15] L. R. Kubendran, H. McMahon, and J. Hubbartt, "Interference Drag in a Simulated Wing-Fuselage Juncture," *NASA Contract. Reports*, 1984.
- [16] Federal Aviation Administration. "Aerodynamics of Flight", *Pilot's Handbook of Aeronautical Knowledge*, 2–5, 2000.
- [17] K. T. Trinh, "On The Critical Reynolds Number For Transition From Laminar To Turbulent Flow," June, 2010,
- [18] C. R. Daubert, "Reynolds Number," *Encycl. Agric. Food, Biol. Eng. Second Ed.*, pp. 1469–1472, 2010.
- [20] B. Gopi Krishna and S. Durga Prasad, "Design and Analysis of Vortex Generators," *Int. J. Mod. Trends Sci. Technol.*, vol. 4, no. 2, pp. 25–31, 2018.
- [21] U. Fernandez-Gámiz, E. Egusquiza, and C. Marika, "Fluid Dynamic Characterization of Vortex Generators and Two-dimensional Turbulent Wakes." *Thesis submitted in partial fulfilment for the degree of Doctor of Philosophy*, Polytechnic University of Catalonia, 2013.
- [22] N. K. Velagapudi, L. N. K., L. N. V. N. Rao, and S. R. Y., "Investigation of Drag and Lift Forces over the Profile of Car with Rearspoiler using CFD," *Int. J. Adv. Sci. Res.*, vol. 1, no. 8, p. 331, 2015.
- [23] Advanced Vehicle Technology, *Adv. Veh. Technol.*, 2002.
- [24] William L. Hosch. (2009). Navier-Stokes Equation, Encyclopedia Britannica. Retrieved, May 24, 2019, from <https://www.britannica.com/science/Navier-Stokes-equation>

- [25] M. Koike, T. Nagayoshi, and N. Hamamoto, "Research on Aerodynamic Drag Reduction," *Mitsubishi Mot. Tech. Rev.*, vol. No. 16, no. 2, pp. 11–16, 2004.
- [26] P. N. Selvaraju, K. M. Parammasivam, S. Shankar, and G. Devaradjane, "Analysis of drag and lift performance in sedan car model using CFD," *J. Chem. Pharm. Sci.*, vol. 7, no. 7, pp. 429–435, 2015.
- [27] S. S. Rajan, H. P, S. Senthilkumar, and P. M. K, "Aerodynamic Drag Reduction on a Sedan Car by Provision of Vortex Generators through Wind Tunnel Studies," *Natl. Conf. Wind Tunn. Test.*, vol. 1, pp. 1–7, 2013.